Giono, G., Gudmundsson, J. T., Ivchenko, N., Mazouffre, S., Dannenmayer, K., Loubère, D., Popelier, L., Merino, M. y Olentšenko, G. (2018). Non-Maxwellian Electron Energy Probability Functions in the plume of a SPT-100 Hall thruster. *Plasma Sources Science and Technology*, 27(1).

DOI: https://doi.org/10.1088/1361-6595/aaa06b

Non-Maxwellian Electron Energy Probability Functions in the plume of a SPT-100 Hall thruster.

G Giono[1,2], J T Gudmundsson[1,3], N Ivchenko[1], S Mazouffre[4], K Dannenmayer[5], D Loubère[6], L Popelier[6], M Merino[7] and G Olentšenko[1]

[1] Department of Space and Plasma Physics, School of Electrical Engineering, KTH-Royal Institute of Technology, Stockholm, Sweden
[2] Leibniz-Institute of Atmospheric Physics (IAP), Kühlungsborn, Germany
[3] Science Institute, University of Iceland, Reykjavik, Iceland
[4] Institut de Combustion Aérothermique Réactivité et Environnement (ICARE), CNRS-University of Orléans, Orléans, France
[5] European Space Research and Technology Centre (ESA/ESTEC), Noordwijk, The Netherlands
[6] Airbus Defense and Space (Airbus-DS), Toulouse, France
[7] Equipo de Propulsión Espacial y Plasmas (EP2), Universidad Carlos III de Madrid (UC3M), Leganés, Spain

E-mail: ggiono@kth.se

Abstract. We present measurements of the electron density, the effective electron temperature, the plasma potential, and the Electron Energy Probability Function (EEPF) in the plume of a 1.5 kW-class SPT-100 Hall thruster, derived from cylindrical Langmuir probe measurements. The measurements were taken on the plume axis at distances between 550 mm and 1550 mm from the thruster exit plane, and at different angles from the plume axis at 550 mm for three operating points of the thruster, characterized by different discharge voltages and mass flow rates. The bulk of the electron population can be approximated as a Maxwellian distribution, but the measured distributions were seen to decline faster at higher energy. The measured EEPFs were studied for best modelled with a general EEPF with an exponent α between 1.2 and 1.5, and their axial and angular characteristics were studied for the different operating points of the thruster. As a result, the exponent α from the fitted distribution was seen to be almost constant as a function of the axial distance along the plume, as well as across the angles. However, the exponent α was seen to be affected by the mass flow rate, suggesting a possible relationship with the plasma density inside the plume. The ratio of the specific heats, the γ factor, between the measured plasma parameters was found to be lower than the adiabatic value of 5/3 for each of the thruster settings, indicating the existence of non-trivial kinetic heat fluxes in the near collisionless plume. These results are intended to be used as input and/or testing properties for plume expansion models in further work.

Submitted to: *Plasma Sources Sci. Technol.*

1. Introduction

Electric propulsion is a solid alternative to classical chemical propulsion for both station keeping and orbit raising of spacecraft, as well as for deep space exploration. Hall thrusters are a type of electric thruster in which heavy atoms, typically noble gas such as Xenon, are ionized and accelerated using an electric field (Goebel & Katz 2008, Martinez-Sanchez & Pollard 1998, Boeuf 2017, Mazouffre 2016). The ejection of the ions provides thrust to the spacecraft; neutralization of those ions is necessary to avoid payload charging and therefore electrons are also ejected from a cathode. Both ions and electrons then form the plasma plume expanding from the thruster exhaust. Understanding the plasma environment created by the electric thruster is crucial in order to avoid issues such as energetic ions sputtering onto the spacecraft, direct contamination due to erosion products or impingement of ions nearby of the spacecraft which can induce perturbing forces and torques. Of particular concern with the use of Hall thrusters is the effect of the highly energetic plasma exhaust plume on the surfaces of the spacecraft, in particular the solar arrays. For these reasons, advanced modelling of the plasma plume is required (Hu & Wang 2017, Sedmik et al. 2005, Boyd & Dressler 2002, Beal et al. 2004, Roussel et al. 1997, Roussel et al. 2008) in order to improve understanding and provide input for optimizing spacecraft design.

However, proper knowledge of the plasma behaviour in this region is still lacking, with a major missing piece being the cooling mechanism of the electrons as the plume expands, both along its axis and angularly off the plume axis. The cooling of the electrons is linked to the absence of local thermodynamic equilibrium in the low-collisionality plume. In a highly collisional plume, adiabatic cooling from the local thermodynamic equilibrium of the electrons would be expected, whereas in a collisionless plume, most electrons are axially confined by the ambipolar electric field and a purely confined electron species would be isothermal. The actual expansion is more complicated than a middle point between the two cases: part of the electrons escape downstream to neutralize the ion beam, and non-monotonic effective potential barriers may exist. Theoretical work is ongoing in order to provide a solution to this problem (Merino et al. 2016, Cichocki et al. 2014, Cichocki et al. 2015) and the presented work aims at providing experimental measurements to support this effort. There have been experimental characterization of Hall thrusters using Langmuir probes, including the very-near-field plume (0 to 200 mm, Kim et al. 1996) and the far-field plume (300 to 500 mm, Dannenmayer et al. 2011, Dannenmayer et al. 2012, Dannenmayer & Mazouffre 2013), but reliable measurements beyond 500 mm are scarce.

This article presents new results from a measurement campaign in which cylindrical Langmuir probes were used to measure the key plasma parameters at distances between 500 mm and 1550 mm from the exit of a SPT-100 (Stationary Plasma Thruster) Hall thruster. The electron density, the effective electron temperature and the Electron Energy Probability Functions were recorded at multiple axial and angular locations inside the plume far-region of the thruster.

2. Experimental apparatus, method and measurements

Measurements were performed inside a large vacuum chamber (2 m in diameter and 4 m in length) using two cylindrical Langmuir probes (0.2 mm diameter, 5 mm length) oriented parallel to ion stream lines. The tip of the probes was made of Tungsten, with an alumina body shielding the rest of the probe. The first cylindrical Langmuir probe was installed on a translation stage, mounted on a rotating arm, allowing for angular scans at distances from 500 to 750 mm to the thruster exit. The second cylindrical Langmuir probe was mounted on a larger translation stage, providing measurements along the plume axis from 850 to 1550 mm. All measurements were performed in the horizontal plane located at the height of the thruster axis (x=0 referring to the exit of the thruster), and recorded using a Keithley 2440 sourcemeter sweeping the probe voltage from -15 V to $+35$ V.

In this article, only measurements performed along the plume axis (from 550 to 1550 mm with respect to the thruster) and angularly from 0.5° to 84.5° (0° being aligned with the thruster axis) at a radial distance of 550 mm are discussed. An overview of the configuration is shown in Figure 1, with the location of the discussed measurements indicated in red. These measurements were recorded for three different operating points of the thruster, where the discharge voltage and the mass flow rate of Xenon were varied: (300 V, 4 mg/s), (300 V, 2 mg/s), and (400 V, 2 mg/s), respectively.

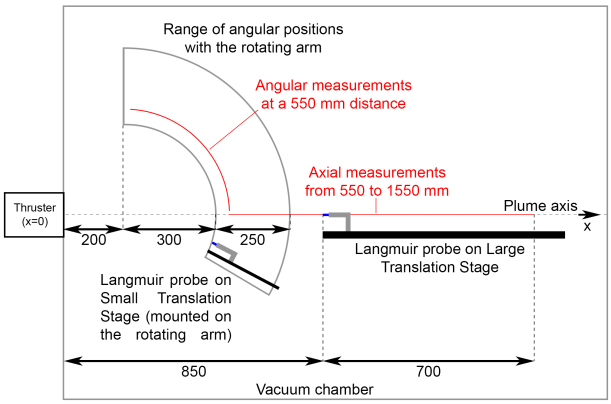

Figure 1. Experimental configuration inside the vacuum chamber. The location of the measurements discussed is shown in red.

The Hall thruster employs magnetic fields to achieve propellant acceleration, however since the plume region studied here was more than 500 mm away from the discharge region, the magnetic field is negligible and the plasma can be considered unmagnetized. The pressure inside the vacuum chamber while running the thruster was below 10^{-4} Torr during all measurements, and below 10^{-6} Torr otherwise. Hence, Xenon neutrals were by far the most abundant element inside the chamber when running the thruster, with number density between 1×10^{18} and 2×10^{18} m^{-3} for a mass flow rate of 2 and 4 mg/s, respectively. This is assuming room temperature and a uniform distribution of the neutrals in the far-plume. The mean free path of an Xenon ion can be calculated based on its charge exchange cross section (Miller et al. 2002) to be around 0.8 m at 2 mg/s and 0.4 m at 4 mg/s. On the other hand, electron collision with neutral can be estimated based on the total scattering cross-section of Xenon (Subramanian & Kumar 1987), which can be seen to vary greatly as a function of energy from 1 eV to 6 eV but becomes constant beyond 6 eV. Based on this, the mean free path of electrons in neutral Xenon is larger than 2 m at 2 mg/s and larger than 1 m at 4 mg/s. Therefore, the plasma inside the plume cannot be considered fully-collisionless, but the average number of collision is not very high either: between 1 and 3 collisions along a 1.5 meter distance for ions, and between 0.5 to 1.5 collisions for electrons. As a consequence of this, the electrons are not in local thermodynamic equilibrium.

The plasma parameters were derived from the Langmuir probe current measurements. First, the plasma potential was determined by locating the maximum of the first derivative of the current $\mathrm{d}I/\mathrm{d}V$, smoothed using a Blackman window convolution (2 V width) to reduce the fluctuation induced by the measurement noise (Magnus & Gudmundsson 2008). The Electron Energy Distribution Function (EEDF) $g_\mathrm{e}(\mathcal{E})$ was then derived by taking the second derivative of the current $\mathrm{d}^2I/\mathrm{d}V^2$ from the plasma potential, following the Druyvesteyn formula (Lieberman & Lichtenberg 2005), using the smoothed $\mathrm{d}I/\mathrm{d}V$. The Druyvesteyn formula is

$$g_\mathrm{e}(\mathcal{E}) = \frac{2m_\mathrm{e}}{e^2 \mathrm{A}} \sqrt{\frac{2e\mathcal{E}}{m_\mathrm{e}}} \frac{\mathrm{d}^2 I}{\mathrm{d}V^2} \tag{1}$$

where m_e is the mass of the electron, e the elementary charge and A the area of the probe. The Electron Energy Probability Function (EEPF) $g_\mathrm{p}(\mathcal{E})$ is obtained as $g_\mathrm{p}(\mathcal{E}) = \mathcal{E}^{-1/2} g_\mathrm{e}(\mathcal{E})$.

The measured EEPFs are presented in Figure 2 along the plume axis and in Figure 3 for angles off the plume axis, at a 550 mm radial distance. For the three operating conditions, one can see the spatial variation of the EEPF and its relation with the plasma parameters, as its amplitude is proportional to the density and its slope to the electron temperature.

The EEPF peaks at an energy between 0 and 2 eV, which decreases slightly with increased distance and larger angle. In addition, the depletion at low-energy below 1 eV is a measurement artifact due to the finite size of the Langmuir probe (Godyak et al. 1992). The noise level can be seen to be about three orders of magnitude lower than the maximum, although values below two orders of magnitude can be seen to be affected by the smoothing of the current derivative.

3. Analysis of the EEPFs

The electron density n_e and effective electron temperature T_eff for each measurement can be calculated by integrating the EEDFs (Lieberman & Lichtenberg 2005), as

$$n_\mathrm{e} = \int g_\mathrm{e}(\mathcal{E})\mathrm{d}\mathcal{E} \qquad T_\mathrm{eff} = \frac{2}{3n_\mathrm{e}} \int \mathcal{E} g_\mathrm{e}(\mathcal{E})\mathrm{d}\mathcal{E} \tag{2}$$

where the effective electron temperature is $T_\mathrm{eff} = \frac{2}{3}\langle\mathcal{E}\rangle$ and $\langle\mathcal{E}\rangle$ is the average electron energy. Note that the measured EEDFs were not truncated at the floating potential energy, as the second derivative of the ion current can be considered negligible (Godyak et al. 1992).

Observations show that the bulk of the electron population has a distribution function close to a Maxwellian (EEPF as a straight line, see Figure 4, fitted on the 2 eV wide region following the EEPF maximum). However, for larger electron energy, the distribution rapidly deviates from this Maxwellian distribution: the measured electron energy probability decreases faster than expected from the main Maxwellian population. Such deviation from a Maxwellian distribution was also observed by other authors (Dannenmayer & Mazouffre 2013, Boswell

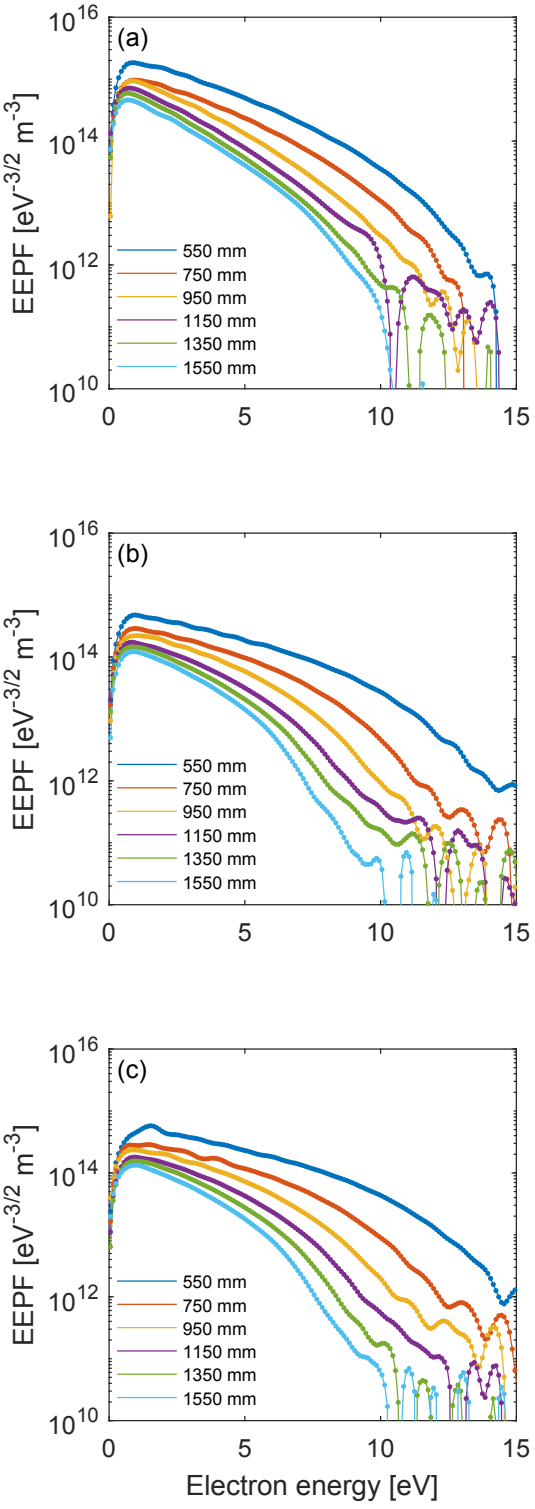

Figure 2. EEPFs measured along the plume axis, for (a) 300 V, 4 mg/s, (b) 300 V, 2 mg/s and (c) 400 V, 2 mg/s. Not every axial measurements are shown.

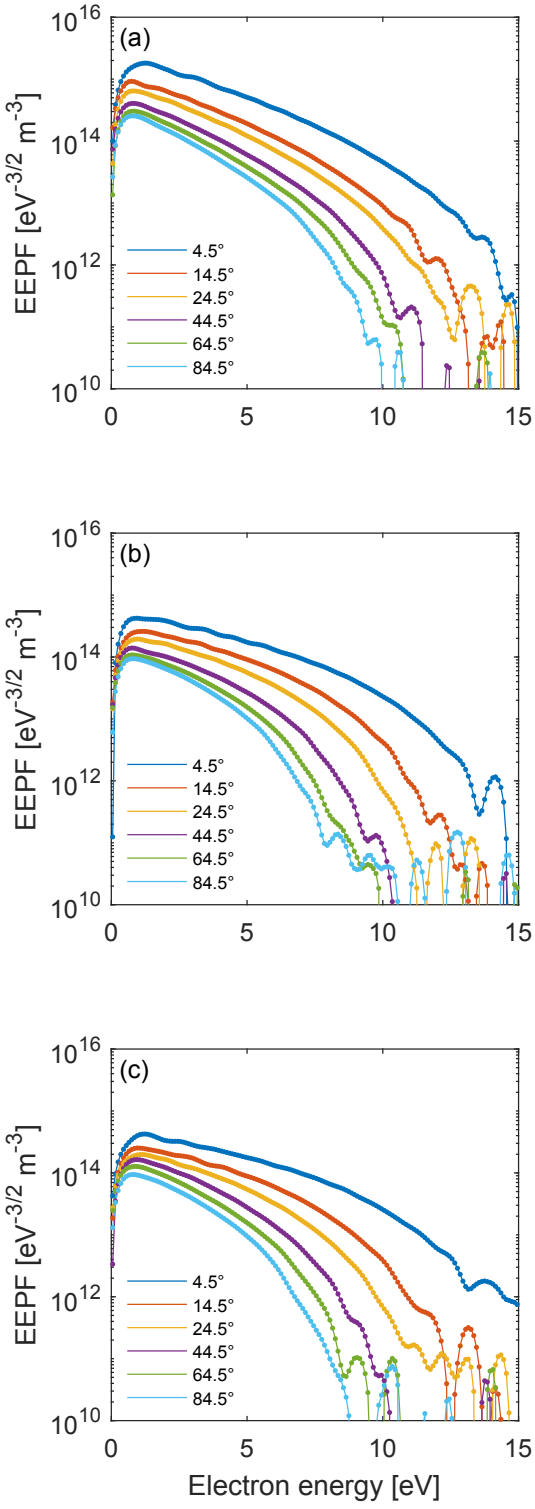

Figure 3. EEPFs measured angularly (at a 550 mm distance from the thruster), for (a) 300 V, 4 mg/s, (b) 300 V, 2 mg/s and (c) 400 V, 2 mg/s. Not every angular measurements are shown.

et al. 2015, Zhang et al. 2016*b*) at distances much closer to the thruster. Note that the observed EEPFs are also different from the convex bi-Maxwellian case described by (Zhang et al. 2016*a*): the depletion observed at higher energy drops faster than for a second Maxwellian distribution.

Further investigation of the non-Maxwellian general case was therefore required. A more general formulation for the EEPF is

$$g_{\rm p}(\mathcal{E}) = n_{\rm e}\frac{3\alpha}{T_{\rm eff}^{\frac{3}{2}}}\frac{\left[2\Gamma\left(\frac{5}{2\alpha}\right)\right]^{\frac{3}{2}}}{\left[3\Gamma\left(\frac{3}{2\alpha}\right)\right]^{\frac{5}{2}}}\exp\left\{-\left[\frac{2\Gamma\left(\frac{5}{2\alpha}\right)}{3\Gamma\left(\frac{3}{2\alpha}\right)}\frac{\mathcal{E}}{T_{\rm eff}}\right]^{\alpha}\right\} \quad (3)$$

where α is an exponent describing the curvature of the EEPF (Rundle et al. 1973, Gudmundsson 2001). This expression is auto-consistent with Equation (2), and reduces to a Maxwellian distribution for α=1, whereas α=2 leads to a Druyvesteyn distribution. A least-square fitting was used to derive the exponent α, as well as the two plasma parameters, from the measured EEPFs. Only the central part of the EEPF was used for this fitting, from its maximum (*i.e.* not including the drop at very low energy due to the finite size of the Langmuir probe) to the noise level (*i.e.* threshold at two orders of magnitude lower than the EEPF maximum). An example of Maxwellian distribution and general distribution fitting is shown in Figure 4.

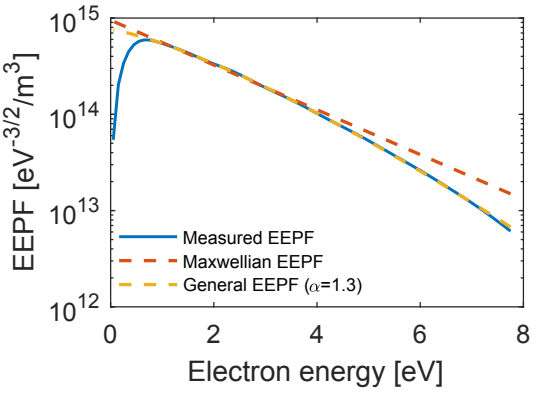

Figure 4. Example of EEPF showing the Maxwellian fitting on the bulk of the distribution, as well as the general fitting. The EEPF is taken along the plume axis at a 1350 mm distance from the thruster exit, for a discharge voltage of 300 V and a mass flow rate of 4 mg/s.

4. Results and discussion

For each of the operating points, three sets of parameters are shown in Figure 5 and Figure 6, as a function of the distance along the plume axis, one derived from the measurements, and two from fittings, with a simple Maxwellian and with the general non-Maxwellian, respectively. The measurement value is obtained from integrating the entire experimentaly determined EEDF. The derived parameters of the bulk Maxwellian distribution provide an overestimate of $n_{\rm e}$ and $T_{\rm eff}$, as the EEPF is observed to decay faster than a Maxwellian at higher energy. On the other hand, the general non-Maxwellian distribution provides very similar plasma parameters as determined from the measurements. Only a small difference can be seen in the electron density, indicating that the loss of low energy electrons observed in the measurement was not significant. All three methods show a similar picture: both electron density and temperature falling off with distance away from the thruster exit. The electron density, shown in Figure 5, at 500 mm depends mainly on the flow rate and is 1.2×10^{16} m^{-3} at 300 V and 4 mg/s. It falls off with distance and is 2.4×10^{15} m^{-3} 1550 mm from the exit as seen in Figure 5(a). The electron density decreases to 3.6×10^{15} m^{-3} at 550 mm from the exit when the flow rate is decreased to 2 mg/s at 300 V. The electron density only increases slightly to 4.5×10^{15} m^{-3} at 550 mm from the exit when the discharge voltage is increased to 400 V while the flow rate is 2 mg/s, as seen in Figure 5(c). At this flow rate, the electron density drops to 5×10^{14} m^{-3} at 1550 mm from the thruster exit. The effective electron temperature seen in Figure 6 is slightly higher for the lower flow rate, or 3.0 eV at 550 mm from the thruster exit at 2 mg/s but drops to 2.4 eV as the flow rate is increased to 4 mg/s while operating at 300 V. In all cases, $T_{\rm eff}$ has dropped to roughly 1.7 eV at 1550 mm from the thruster exit. These values are consistent with other studies with a SPT-100 thruster such as (Dannenmayer et al. 2011). For reference, Figure 7 gives the plasma potential along the plume axis, derived from the maximum of the smoothed first derivative of the current. The plasma potential can be seen to drop from around 13 V at 550 mm from the thruster exit to about 7 V at 1550 mm. One can see that a small offset in the plasma potential curve can be seen between a discharge voltage of 300 V and 400 V, with $V_{\rm p}$ at 400 V being slightly larger than at 300 V. Finally, one can notice that the shape of the spatial variation of $V_{\rm p}$ for a larger mass flow rate of 4 mg/s is slightly different compared to 2 mg/s.

Figure 8 shows the spatial dependence of the exponent α. The exponent α has values between 1.2 and 1.5, which is in-between Maxwellian and Druyvesteyn distributions. Note that this result for the exponent α could be a consequence of the experimental conditions, *i.e.*, having a much higher neutral density in the background than in space. This will expectedly make the EEPF approach the Druyvesteyn distribution. In the better vacuum of space, the results could be different. Nevertheless, the axial and angular variations of the exponent can be discuss meaningfully. Although no significant trends

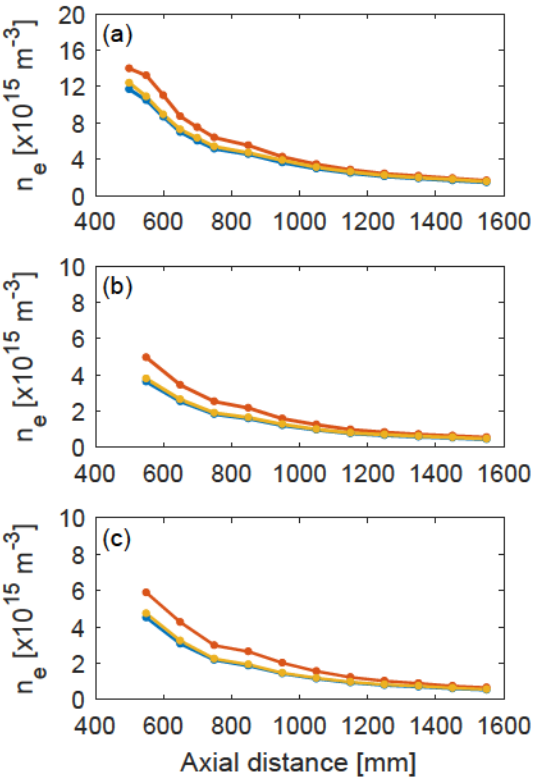

Figure 5. Electron density along the plume axis for (a) 300 V, 4 mg/s, (b) 300 V, 2 mg/s and (c) 400 V, 2 mg/s. Blue solid line shows the density obtained from integrating the EEDF measurements, red solid line from the Maxwellian distribution and yellow solid line from the general distribution fitting.

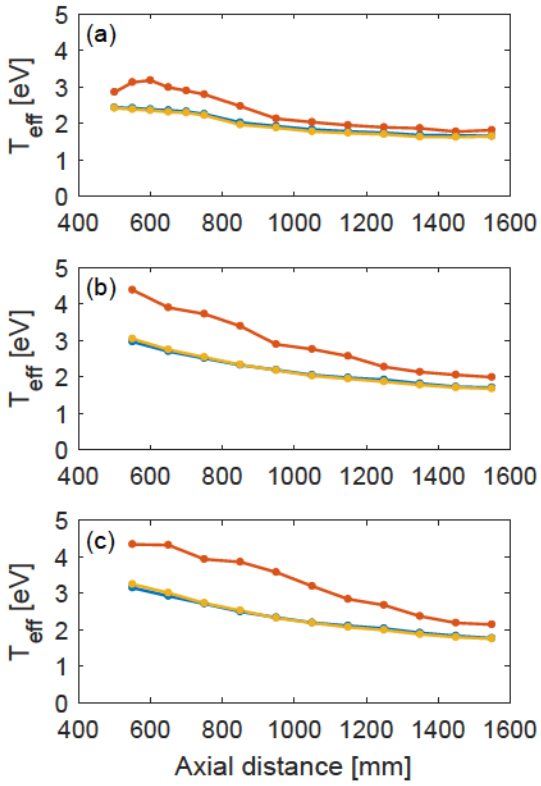

Figure 6. Effective electron temperature along the plume axis for (a) 300 V, 4 mg/s, (b) 300 V, 2 mg/s and (c) 400 V, 2 mg/s. Blue solid line shows the temperature obtained from integrating the EEDF measurements, red solid line from the Maxwellian distribution and yellow solid line from the general distribution fitting.

are observed along the plume axis or across the angles, a clear difference is seen depending on the mass flow rate of the thruster, which might suggest a relation between rate of high-energy electrons loss and the plasma density inside the plume.

Establishing a relation between the electron temperature and plasma density is important for the fluid-type models of the plume. In the adiabatic case, the electron density and the electron temperature can be related by the ratio of specific heats γ (Boyd & Dressler 2002) as in

$$\left(\frac{n_e}{n_e^*}\right)^{\gamma} = \left(\frac{T_{\text{eff}}}{T_{\text{eff}}^*}\right)^{\frac{\gamma}{\gamma-1}} \tag{4}$$

where $*$ indicates a reference state. In a collisional gas plume, local thermodynamic equilibrium is expected and a γ value of $5/3$ is anticipated due to adiabatic cooling. However, in a nearly-collisionless plasma plume, one cannot invoke local thermodynamic equilibrium condition and no simple physical argument leads to $5/3$ in a general collisionless plasma expansion; the kinetic response of the electrons must be studied in detail. A $\gamma < 5/3$ in an otherwise isentropic expansion indicates the existence of non-trivial electron kinetic heat-fluxes. The tendency in a collisionless, confined

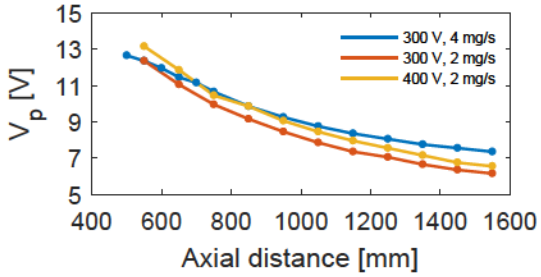

Figure 7. Plasma potential along the plume axis for the three operating points of the thruster.

population is for heat fluxes to make the population near-isothermal (*i.e.* Boltzmann relation). For a partially confined population, $1 < \gamma < 5/3$ is expected. Best fits of the γ parameter between the electron density and effective electron temperature obtained from the measured EEDFs are shown in Figure 9. For each operating point of the thruster, the derived γ is lower than the adiabatic value. Similar values were reported by (Dannenmayer & Mazouffre 2013, Boswell et al. 2015, Zhang et al. 2016*b*), and indicate that the medium is far from thermodynamic equilibrium and the existence of non-trivial kinetic heat-fluxes. The γ

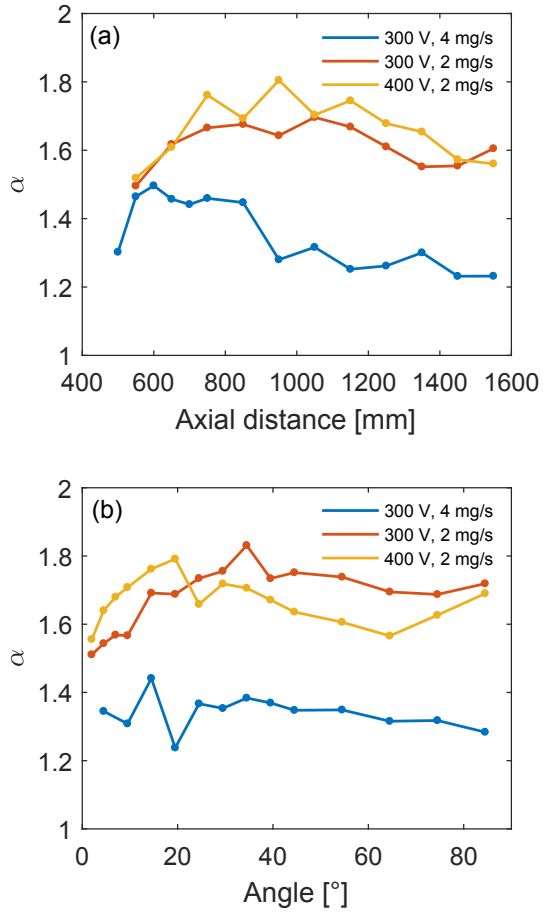

Figure 8. Axial (a) and angular (b) variation of the exponent α for each of the three operating points of the thruster.

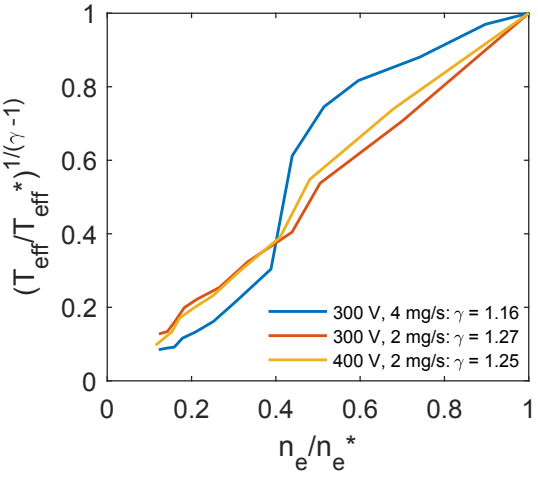

Figure 9. Best fit of the γ factor between the measured n_e and T_{eff} along the axis. Values are normalized to a common reference point (axial measurement at 550 mm).

factor was also derived for the parameters of the fitted Maxwellian distribution and similar values between 1.2 and 1.5 were obtained, indicating that even the bulk of the electron population does not follow an adiabatic cooling law.

5. Conclusion

EEPF measurements in the far-plume of a SPT-100 Hall thruster revealed a loss of high energy electrons compared to the Maxwellian electrons from the bulk of the plasma. The measured EEPFs were best represented by a general electron energy probability function with an exponent α. Best fit for the exponent was between 1.2 and 1.5, placing the measured distributions between a Maxwellian and a Druyvestyn distributions. The exponent α was roughly constant as a function of axial distance and angle, but a clear dependence on the mass flow rate of the thruster was observed, indicating a possible dependence on the plasma density inside the plume. A γ parameter around 1.2 was found to link the electron density to the electron temperature, which is smaller than the value for adiabatic cooling of 5/3. This suggests an electron population far from the thermodynamic equilibrium. Based on the background pressure, the number of collisions with neutral Xenon atoms experienced by a Xenon ion and an electron was respectively estimated to be between one and three, and around one. Such regime is not collisionless, but not highly collisional either.

The electron cooling in a nearly-collisionless plasma is far from trivial, but the presented considerations on the EEPFs properties could serve as input and/or testing parameters for the modelling of the plume expansion.

Acknowledegment

This work was performed in the framework of the "Model and Experimental validation of spacecraft-thruster Interactions (erosion) for electric propulsion thrusters plumes" (MODEX) project. MODEX is a collaboration between Airbus-DS, ESA, UC3M, ONERA, CNRS-ICARE and KTH aiming to provide a better understanding of the plasma properties in the far-plume of a Hall thruster. The project aimed at providing experimental measurements to better constrain the modelling, and therefore includes both the theoretical/modelling aspect (UC3M and ONERA) and the experimental aspect (KTH, CNRS, ESA and Airbus-DS). The test campaign was conducted at ESA/ESTEC in April-May 2017, using a SPT-100 Hall thruster provided by Airbus-DS. G. Giono and J. T. Gudmundsson were partially supported by the Swedish Government Agency for Innovation Systems (VINNOVA) contracts no. 2016-04094 and 2014-0478, respectively.

References

Beal B E, Gallimore A D, Haas J M & Hargus W A 2004 *Journal of Propulsion and Power* **20**(6), 985–991.

Boeuf J P 2017 *Journal of Applied Physics* **121**(1), 011101.

Boswell R W, Takahashi K, Charles C & Kaganovich I D 2015 *Frontiers in Physics* **3**, 14.

Boyd I D & Dressler R A 2002 *Journal of Applied Physics* **92**(4), 1764–1774.

Cichocki F, Merino M & Ahedo E 2014 *in* 'Propulsion and Energy Forum, 50nd AIAA/ASME/SAE/ASEE Joint Propulsion Conference' Cleveland, USA pp. AIAA 2014–3828.

Cichocki F, Merino M, Ahedo E, Hu Y & Wang J 2015 *in* '34th International Electric Propulsion Conference' Hyogo-Kobe, Japan pp. IEPC–2015–420.

Dannenmayer K, Kudrna P, Tichý M & Mazouffre S 2011 *Plasma Sources Science and Technology* **20**(6), 06512.

Dannenmayer K, Kudrna P, Tichý M & Mazouffre S 2012 *Plasma Sources Science and Technology* **21**(5), 055020.

Dannenmayer K & Mazouffre S 2013 *Plasma Sources Science and Technology* **22**(3), 035004.

Godyak V A, Piejak R B & Alexandrovich B M 1992 *Plasma Sources Science and Technology* **1**(1), 36 – 58.

Goebel D M & Katz I 2008 *Fundamentals of Electric Propulsion: Ion and Hall Thrusters* John Wiley & Sons Hoboken, New Jersey.

Gudmundsson J T 2001 *Plasma Sources Sci. Technol.* **10**, 76–81.

Hu Y & Wang J 2017 *Physics of Plasmas* **24**(3), 033510.

Kim S W, Foster J & Gallimore A 1996 *in* '32nd AIAA/ASME/SAE/ASEE Joint Propulsion Conference and Exhibit, Lake Buena Vista, FL' pp. AIAA Paper 96–2972.

Lieberman M A & Lichtenberg A J 2005 *Principles of Plasma Discharges and Materials Processing* second edn John Wiley & Sons New York.

Magnus F & Gudmundsson J T 2008 *Review of Scientific Instruments* **79**(7), 073503.

Martinez-Sanchez M & Pollard J E 1998 *J. Propulsion Power* **14**, 688–699.

Mazouffre S 2016 *Plasma Sources Sci. Technol.* **25**, 033002.

Merino M, Proux A, Fajardo P & Ahedo E 2016 *in* 'Propulsion and Energy Forum, 52nd AIAA/SAE/ASEE Joint Propulsion Conference' Salt Lake City pp. AIAA 2016–5037.

Miller J S, Pullins S H, Levandier D J, Chiu Y & Dressler R A 2002 *Journal of Applied Physics* **91**(3), 984–991.

Roussel J F et al. 1997 *in* 'Second European Spacecraft Propulsion Conference' ESTEC, Noordwijk, The Netherlands pp. 517–522.

Roussel J F et al. 2008 *IEEE Transactions on Plasma Science* **36**, 2360–2368.

Rundle H W, Clark D R & Deckers J M 1973 *Canadian Journal of Physics* **51**(2), 144–148.

Sedmik R, Scharlemann C, Tajmar M, González del Amo J, Hilgers A, Estublierk D, Noci G, Capacci M & Koppel C 2005 *in* '29th International Electric Propulsion Conference' Princeton University pp. IEPC–2005–214.

Subramanian K P & Kumar V 1987 *J. Phys. B: At. Mol. Phys* **20**, 5505–5515.

Zhang Y, Charles C & Boswell R 2016*a* *Astrophysical Journal* **829**(1), 10.

Zhang Y, Charles C & Boswell R 2016*b* *Physical Review Letters* **116(2)**, 025001.